Journal of Neurochemistry, 2005, **92**, 1228–1242 doi:10.1111/j.1471-4159.2004.02956.x

Role of the autophagic-lysosomal system on low potassium-induced apoptosis in cultured cerebellar granule cells

Nadia Canu,*,† Roberta Tufi,* Anna Lucia Serafino,† Giuseppina Amadoro,† Maria Teresa Ciotti† and Pietro Calissano*,†

**Dipartimento di Neuroscienze, Facoltà di Medicina e Chirurgia, Università di Tor Vergata, Roma, Italia*
†*Istituto di Neurobiologia e Medicina Molecolare C.N.R., Roma, Italia*

Abstract

Apoptotic and autophagic cell death have been implicated, on the basis of morphological and biochemical criteria, in neuronal loss occurring in neurodegenerative diseases and it has been shown that they may overlap. We have studied the relationship between apoptosis and autophagic cell death in cerebellar granule cells (CGCs) undergoing apoptosis following serum and potassium deprivation. We found that apoptosis is accompanied by an early and marked proliferation of autophagosomal–lysosomal compartments as detected by electron microscopy and immunofluorescence analysis. Autophagy is blocked by hrIGF-1 and forskolin, two well-known inhibitors of CGC apoptosis, as well as by adenovirus-mediated overexpression of Bcl-2. 3-Methyladenine (3-MA) an inhibitor of autophagy, not only arrests this event but it also blocks apoptosis. The neuroprotective effect of 3-MA is accompanied by block of cytochrome *c* (cyt *c*) release in the cytosol and by inhibition of caspase-3 activation which, in turn, appears to be mediated by cathepsin B, as CA074-Me, a selective inhibitor of this enzyme, fully blocks the processing of pro-caspase-3. Immunofluorescence analysis demonstratesd that cathepsin B, normally confined inside the lysosomal-endosomal compartment, is released during apoptosis into the cytosol where this enzyme may act as an execution protease. Collectively, these observations indicate that autophagy precedes and is causally connected with the subsequent onset of programmed death.

Keywords: apoptosis, autophagy, caspase activation, cathepsin B, cerebellar granule neurons, neurodegeneration.
J. Neurochem. (2005) **92,** 1228–1242.

Extensive and premature cell loss in specific neuronal populations by programmed cell death (PCD) is the main pathological hallmark of neurodegenerative diseases (Jellinger and Stadelmann 2000). Although PCD can manifest in many forms, two major kinds of PCD have been proposed (Schwartz *et al*. 1993; Zakeri *et al*. 1995). Type I PCD, or classical apoptosis, is a highly controlled process. It involves a series of well-characterized morphological changes that include loss of cell volume, chromatin condensation, cell blebbing and nuclear fragmentation. At the biochemical level, a cohort of proteases termed caspases contributes to the execution phase of this process (Hengartner 2000).

Type II PCD, on the other hand, is morphologically characterized by increased autophagy and early destruction of the cytoplasm, which either precedes nuclear pyknosis or occurs in its absence (Schweichel and Merker 1973; Clarke 1990; Zakeri *et al*. 1995).

Autophagy consists of a rate-limiting sequestration of cytoplasmic material into double-membrane, autophagic vacuoles derived from the endoplasmic reticular membranes. The vacuole that is formed (the autophagosome)

Received August 3, 2004; revised manuscript received October 23, 2004; accepted November 1, 2004.

Address correspondence and reprint requests to Nadia Canu, Istituto di Neurobiologia e Medicina Molecolare, Consiglio Nazionale delle Ricerche, V. le Marx 15, 00137 Roma, Italia.
E-mail: n.canu@inmm.cnr.it or nadiacanu@tiscalinet.it

Abbreviations used: Ac-DEVD-MCA, Ac-Asp-Glu-Val-Asp-7-amido-4-methylcoumarin; Ac-VEID-MCA, Ac-Val-Glu-Ile-Asp-7-amido-methylcoumarin; CA074-Me, L-*trans*-epoxysuccinyl-Ile-Pro-OH propylamide-methyl ester; CGCs, cerebellar granule cells; DIV, days *in vitro*; ERK, extracellular signal-regulated kinase; JNK, c-Jun N-terminal kinase; 3-MA, 3-methyladenime; MBP, Millonig's phosphate buffer; MDC, monodansylcadaverine; MOI, multiplicity of infection; PBS, phosphate buffer saline; PCD, programmed cell death; PI-3K, phosphatidylinositol-3-kinase; S–K25, culture cell medium containing 25 mM of potassium and without serum; S–K5, culture cell medium containing 5 mM of potassium and without serum; TRITC, tetramethyl-rhodamine-isothiocyanate; z-FA-fmk, benzyloxycarbonyl-Phe-Ala fluoromethyl ketone; zVAD-fmk, benzyloxy-carbonyl-Val-Ala-Asp-fluoromethylketone.

fuses with a prelysosomal compartment where degradation, by lysosomal enzymes, occurs (Klionsky and Emr 2000). This pathway is known to be important in normal cellular homeostasis for the replacement of obsolete organelles and proteins, and in the maintenance of cell function during periods of nutrient deprivation. However, recent studies have shed light on the importance of autophagy in both normal development (Schwartz *et al*. 1993; Zakeri *et al*. 1995) and in pathological conditions (Jeffrey *et al*. 1992; Stefanis *et al*. 2001).

In this latter regard, the vigorous activation of both the neuronal lysosomal system and cellular pathways converging on the lysosomes are prominent neuropathological features anticipating the cell shrinkage in Alzheimer's disease, Huntington disease, scrapie and Creutzfeldt–Jakob disease (CJD; Nixon *et al*. 2001).

Although apoptosis and autophagy are morphologically distinct forms of programmed cell death, recent evidence has suggested that autophagy may coexist with apoptosis (Hengartner 2000) or may precede it in a process that is induced by apoptotic stimuli (Xue *et al*. 1999; Guimaraes *et al*. 2003). Several autophagy-associated proteins, such as cathepsin D, APG5 and cathepsin B are involved in different paradigms of apoptosis *in vitro* (Deiss *et al*. 1996; Levy-Strumpf and Kimchi 1998; Isahara *et al*. 1999; Foghsgaard *et al*. 2000; Guicciardi *et al*. 2000; Kagedal *et al*. 2001). To date the relationship between these two forms of cell death is not known.

We have investigated this relationship in CGCs undergoing apoptosis following serum and potassium withdrawal.

Our study revealed that serum and potassium depletion triggers autophagosome proliferation and points to cathepsin B as a possible mediator of caspase-activation in CGCs undergoing apoptosis.

Materials and methods

Ac-Asp-Glu-Val-Asp-7-amido-4-methylcoumarin (Ac-DEVD-MCA) (00000-3-methyladenine) and Ac-Val-Glu-Ile-Asp-7-amido-methylcoumarin (Ac-VEID-MCA) was from Biomol (Plymouth Meeting, PA, USA). MOCAc-Gly-Lys-Pro-Ile-Leu-Phe-Phe-Arg-Leu-Lys (Dnp) gamma-NH2 was from Peptide International (Louisville, KY, USA). Z-Arg-Arg-MCA was from Sigma (St. Louis, MO, USA). 3-Methyladenine (3-MA), Monodansylcadaverine (MDC), Pepstatin A and forskolin were from Sigma. CA074-Me, zFA-fmk and zVAD-fmk were from Calbiochem (La Jolla, CA, USA). Rabbit-anti-cleaved caspase-3 (Asp175); anti-phospho Akt (Ser473); anti-phospho c-jun; anti-pan jun; anti-*p*-p38; anti-ERK1/2 and anti-*p*-ERK1/2 were from Cell Signalling Technology (New England Biolabs Ltd, Beverly, MA, USA). Rabbit anti-phospho-pan-JNK, sheep anti-cytochrome *c* and mouse anti-β-actin and anti-tubulin were from Sigma-Aldrich. The rabbit anti-rat cathepsin B Ig was a gift of Dr John S. Mort (McGill University, Montreal, Quebec, Canada). The rabbit anti-LC3 Ig was a gift of Dr T. Yoshimori (Department of Cell Biology, National Institute for Basic Biology, Okazaki, Japan). Mouse anti-Lamp-1 was from StressGen Biotechonologies Corp (Victoria, BC, Canada). Mouse anti-COX-IV was from Molecular Probes, Eugene, OR, USA. Human recombinant IGF1 (hrIGF1) was from Boheringer GmbH, Mannheim, Germany.

Cell cultures

Cultures enriched in granule neurons were obtained from dissociated cerebella of 8-day-old Wistar rats (CGC; Charles River, Calco, Italy), as described by Levi *et al*. (1984). Cells were plated in basal medium Eagle (BME; Life Technologies, Gaithersburg, MD, USA) supplemented with 10% fetal bovine serum, 25 mM KCl, and 2 mM glutamine (Life Technologies, Gaithersburg, MD, USA) on dishes (Nunc, Roskilde, Denmark) coated with poly-L-lysine. Cells were plated at 2.5×10^6 per 35 mm dish or 7×10^6 per 60 mm dish. 1β-Arabinofuranosylcytosine (10 μM) was added to the culture medium 18–22 h after plating to prevent proliferation of non-neuronal cells.

Induction of apoptosis

Cultures at 6–7 days *in vitro* (DIV) were washed two times and switched to serum-free BME containing 5 mM KCl (S–K5) supplemented with glutamine and gentamicin. Control cells were washed with BME and maintained in serum-free medium containing 25 mM KCl (S–K25) (D'Mello *et al*. 1993).

Assessment of neuronal viability

Viable CGCs were quantified by counting the number of intact nuclei in a haemacytometer, after lysing the cells in detergent-containing solution (Soto and Sonnenschein 1985; Volontè *et al*. 1994). This method has been shown to be reproducible and accurate and to correlate well with other methods of assessing cell survival-death (Stefanis *et al*. 1997; Stefanis *et al*. 1999). Cell counts were performed in triplicate and are reported as means ± SEM. The data are expressed as the percentage of intact nuclei in the control cultures at each time point. Viable CGCs were also quantified by the MTT tetrazolium salt assay (Manthrope *et al*. 1986) to ensure that the nuclear counts reflected functionally active neurons. Briefly, MTT tetrazolium salt (0.25 mg/mL) was added to neurons grown in 24-well plates and incubated for 1–2 h at 37°C. The reaction media were then gently aspirated, and isopropanol containing 0.08 M HCl was added to solubilize the formazan product. Formazan/isopropanol mixtures were then transferred to 96-well plates and quantified using Multiskan plate reader at 570 nm (Labsystem Multiskan MCC/340 (Labsystems, Helsinki, Finland)). Moreover, Hoechst nuclear staining was used to detect typical chromatin changes (Hoetchst 33258, Sigma, St. Louis, MO, USA). Cells were fixed with phosphate-buffered saline (PBS) containing 4% paraformaldehyde for 20 min, permeabilized with 0.1% Triton X-100-Tris/Cl, pH 7.5 for 5 min, then washed two times with PBS. After incubation with Hoechst 33258 (0.5 mg/mL in PBS), neurons were washed two times with PBS. Coverslipes were photographed using UV by microscope; apoptotic neurons were characterized by scoring condensed nuclei.

Overexpression of Bcl-2 in cerebellar granule cells

Four days after plating, control adenovirus (Ad-βgal) or adenoviral GFP-Bcl-2 (provided by Dr Marco Crescenzi, ISS, Roma) at 30 multiplicity of infection (MOI) were used to transduce CGCs as described by Amadoro *et al*. 2004. CGCs were then further cultured up to 6 DIV when experiments were performed.

Transmission electron microscopy (TEM)

Neurons were fixed, at 4°C for 1 h with 2.5% glutaraldhyde in 0.1 M Millonig's phosphate buffer (MPB; to obtain 100 mL, mix 32 mL 2 M sodium dihydrogen orthophosphate, 14 mL 2 M disodium hydrogen orthophosphate, 50 mL double-distilled water, pH 7,4) containing 2% sucrose, and then post-fixed for 1 h at 4°C with 1% OsO_4 in the same buffer. After washing in MPB cells were dehydrated in ascending ethanol concentrations and embedded in Spurr epoxy resin (Agar Scientific Ltd., Stansted, UK). Ultrathin sections were stained with uranyl acetate and lead citrate and observed under a Philips CM12 transmission electron microscope operating at 80 kV.

Visualization of MDC-labelled vacuoles

Visualization of MDC labelled vacuoles were performed as described by (Biederbick *et al*. 1995). In brief, autophagic vacuoles were labelled with 50 μM monodansylcadaverine (MDC) by incubating neurons grown of coverslips at 37°C for 10 min. After incubation, cells were washed four times with PBS, fixed in 4% paraformaldehyde (w/v in PBS) for 15 min. After fixation, cells were washed three times with PBS and analysed using an Olympus optical microscope equipped with a filter system (excitation filter, 340–380 nm, barrier filter, 430 nm).

Immuofluorescence

CGCs were fixed with for 15 min at 22°C, washed in PBS, pH 7.5, and then permeabilized with 0.1% Triton X-100 and Tris/Cl, pH 7.5, for 5 min. The coverslips were treated with polyclonal antibody against LC3 (1 : 100) and Lamp-1 (1 : 300) or with polyclonal antibody against cathepsin B (1 : 600) or with polyclonal antibody against cytochrome *c* (1 : 600) in a moist chamber overnight at 4°C, rinsed in PBS, and stained with FITC and/or tetramethyl-rhodamine-isothiocyanate (TRITC)-conjugated secondary antibodies (Sigma) for 30 min. Nuclei were stained with Hoechst 33528.

Confocal Laser Scanning Microscopy (CLSM)

Fluorescently labelled samples were imaged by a confocal LEICA TCS 4D microscope (Leica, Heidelberg, Germany) equipped with 100 × 1.3–0.6 oil-immersion objective (optical section, 0.5, 1 μM). Images of double-labelled samples were recorded with simultaneous excitation and detection of both dyes to ensure proper image alignment. The excitation and emission wavelengths were 488 nm and 510 nm, respectively, for FITC-labelling, and 568 nm and 590 nm, respectively, for TRITC-labelling. Optical sections were stereopaired and reconstituted in three dimensions. To correct for possible cross-talk resulting from overlapping excitation and emission spectra of the dyes used, when necessary, recorded images were corrected using the MULTICOLOR analysis package software by Leica.

Nucleosomal formation assay

Nucleosomal formation was determined by quantitative *in vitro* determination of cytoplasmatic histone-associated-DNA-fragments (Cell Death Detection ELISA PLUS, Roche) according to the manufacturer's recommendation. Nucleosomal formation was measured after 12 h of apoptosis induction in the absence or in the presence of 3-MA. Results are expressed as 'enrichment factor' obtained according to the formula: $(OD_{experimental\ point} - OD_{background})/(Od_{control\ point} - OD_{Background})$. Background consists in OD from ELISA plate dishes where cellular extracts were omitted; 'control point' refers the to basal level of apoptosis, i.e. nucleosomes present in cultures maintained in S–K25.

Proteolytic activities of cathepsin B and D

CGCs were lysed in 50 mM Tris/HCl, pH 7.5, 0.15 M NaCl, and 1% Triton for 30 min on ice and then centrifuged at 1250 *g* for 20 min. The activity of cathepsin B was assayed using the z-Arg-Arg-MCA (Sigma) as substrate according to the method of Barret and Kirschke 1981), while that of cathepsin D was assayed using the fluorogenic substrate MOCAc-Gly-Lys-Pro-Ile-Leu-Phe-Phe-Arg-Leu-Lys (Dnp) gamma-NH2 (Peptides International) as described by Yasuda *et al*. (1999).

Measurement of cytosolic cathepsin B activity

To measure cathepsin B activity in the cytosol, cytosolic fractions were prepared as described previously (Nakayama *et al*. 2002) with minor modifications. Pellets were resuspended in extraction buffer (250 mM sucrose, 50 mM HEPES, 1 mM pefablock and 10 mg/mL leupeptin). After 10 min on ice, neurons were lysed with a glass dounce homogenizer with 10 strokes, followed by centrifugation at 750 *g* for 10 min at 4°C to remove nuclei and unbroken cells. Supernatants were then centrifuged at 15 000 *g* for 30 min to remove lysosomes and mitochondria. The resultant supernatants were further centrifuged at 100 000 *g* for 1 h at 4°C and the final supernatants (cytosolic fractions) were collected. Cathepsin B activity was estimated as described above according to the method of Barret and Kirsche (1981).

Fluorogenic peptide substrate assay for caspase activities

Caspase-3 activity was measured, as described previously (Canu *et al*. 2000). After 8 h of incubation in S-K5, 500 000 granule cells were washed once with PBS and lysed in 100 μL of buffer A (10 mM HEPES pH 7.4, 42 mM KCl, 5 mM $MgCl_2$, 1 mM dithiothreitol (DTT), and 1 mM PMSF, 0.5% 3-[(3-cholamidopropyl) dimethylammonio]-1-propanesulphonic acid (CHAPS), and 1 mg/mL leupeptin). Lysate (25 μL) was combined with 75 μL of buffer B (25 mM HEPES, 1 mM EDTA, 0.1% CHAPS, 10% sucrose, and 3 mM DTT pH 7.5) containing 30 μM Ac-DEVD-MCA and incubated for 20 min at 22°C. Caspase-6 activity was measured, as described previously (Allsopp *et al*. 2000), combining 40 μL of lysate from buffer A with 200 μL of buffer B (25 mM HEPES/KOH pH 7.5, 50 mM NaCl, 1 mM EDTA, 5 mM EGTA, 2 mM $MgCl_2$ 0.1% CHAPS, 10% sucrose, and 10 mM DTT) containing 20 μM of caspase-6 fluorogenic substrate Ac-VEID-MCA and incubated at 37°C for 30 min. Fluorescence was measured at an excitation of 380 nm and an emission of 460 nm wavelengths using a Packard Fluorocount microplate reader (Packard Bioscience Company, Meriden, CT, USA).

Western blot analysis

Equal amounts of proteins were subjected to SDS–PAGE on 10% gels. After electroblotting to nitrocellulose (Hybond-C), proteins were visualized using appropriate primary antibodies. All primary antibodies were diluted in 0.5% (w/v) non-fat dry milk and incubated with the nitrocellulose blot overnight at 4°C. Incubation with secondary peroxidase-coupled anti-mouse or anti-rabbit Igs

was performed at room temperature for 45 min. Immunoreactivity was detected by the enhanced chemiluminescence (ECL) reaction (Amersham).

RT-PCR experiments

Total RNA (3 μg/μL), extracted from CGCs and PC12 was retrotranscribed, using random hexamers, by Molony murine leukaemia virus reverse transcriptase.

The template produced from the RT reaction was amplified using the following primers: 5′-GATGGCCCAGAACCTTGTGG-3′ sense and 5′-CCAGCCGGAGGTTGAATGTC-3 antisense, which would be expected to produce PCR product sizes of 383 base pairs (bp). The nested PCR was performed with the sense 5′-CAAGGTGG-CTCAGGCAGTGA-3′ starting at 879 and the antisense primer above, which would be expected to produce a PCR product of 325 bp. For the PCR reaction, 29 μL of H_2O, 5 μL of 10× PCR buffer, 4 μL of $MgCl_2$ (25 mM), 1 μL of dNTP (10 mM of each), 0.5 μL of *Taq* DNA polymerase (5 U/μL), 0.25 μL of both the relevant oligonucleotide primers (50 μM), and 5 μL cDNA reaction (or, for the control, 5 μL of the RT reaction in which reverse transcriptase had been omitted) were added to each tube to give a final volume of 50 μL. The PCR reaction was run on a GeneAmp PCR system 9600 (Perkin-Elmer/Cetus, Norwalk, CT, USA) at 94°C for 1 min, followed by 40 cycles of 94°C for 30 s, 56°C for 30 s, 72°C for 45 s.

Results

Activation of autophagy in CGCs undergoing apoptosis

Rat CGCs can be induced to undergo apoptosis if the potassium concentration is reduced to 5 mM (K5) and serum is removed (S–) after a period of initial growth in 25–30 mM potassium (K25) and serum (S+) (Galli *et al*. 1995; D'Mello *et al*. 1993 Gallo *et al*. 1985). This form of cell death has been described as apoptotic or PCD type 1 because it is dependent on macromolecular synthesis, is accompanied by DNA fragmentation and is temporarily prevented by the pan caspase-inhibitor, z-VAD-fmk (D'Mello *et al*. 1993; Nardi *et al*. 1997; Canu *et al*. 2000). In fact, we found that this substance delays but does not irreversibly block death of these neurons (N. Canu, unpublished observations). This observation raised the possibility that KCl and serum deprivation may trigger an alternative mechanism of cell death as also suggested by other reports (Miller *et al*. 1997; Tanabe *et al*. 1998). To gain insights into this issue, we examined the ultrastucture of CGCs during the commitment phase (0–6 h) (Galli *et al*. 1995) of apoptosis. As visualized by electron microscopy the morphology of control CGCs included big nuclei with fine dispersed chromatin and a normal complement of healthy mitochondria and endoplasmic reticulum (Figs 1a and b, arrow). In contrast, CGCs exposed to 6 h of serum and KCl deprivation displayed large electron-dense membranous whorls and vacuoles in the cytoplasm and in the neurites. Vacuoles were more abundant in neurons with the earliest apoptotic alteration in nuclear morphology (e.g. condensation of nuclear morphology into electron dense packed material along the nuclear membrane) and with condensed mitochondria and cytoplasm (Figs 1c, e and f) (Hacker 2000). These vacuoles, ≈ 600 Å in diameter, resembled autophagosomes based on the presence of a double membrane and the nature of the contents, which appeared to consist of cytoplasmic structures at different stages of digestion (Fig. 1d). In apoptotic neurons, at 6 h of apoptosis, the number of autophagosomes was 6 ± 1.45 (mean ± SEM) per cell section, while in control neurons the number of vacuoles was 1.3 ± 0.97 (mean ± SEM). As apoptosis progressed in these cultures the number of autophagosome declined. This could reflect their progressive fusion with lysosomes (not shown).

As a first attempt to follow the autophagic activation during the progression of apoptosis, we used the autofluorescent drug monodansylcadaverine (MDC), a specific autophagolysosome marker (Biederbick *et al*. 1995; Munafo and Colombo 2001). As shown in Fig. 1g, control neurons displayed very faint, dispersed basal MDC staining, but serum and KCl deprived neurons appeared to be filled progressively with rounded MDC labelled structures throughout the soma and neurites (Fig. 1g). This vacuolization, which appears very shortly after the apoptotic stimulus, was also detected by immunofluorescence analysis using an antibody against LC3 (microtubule-associated protein light chain 3) a selective marker of autophagosomes (Kabeya *et al*. 2000). LC3, the mammalian homologue of the yeast autophagy gene *Aut7/Apg8*, is a soluble cytoplasmic protein in cells growing in normal conditions, but it becomes membrane associated under starving conditions. In control CGCs, the LC3 immunofluorescence pattern was diffuse but became punctate after 1–3 h of KCl and serum withdrawal (Fig. 2), similar to findings reported previously (Kabeya *et al*. 2000).

The LC3 punctuate staining was present only in the early phase of apoptosis and, as reported previously (Kabeya *et al*. 2000) never overlapped with Lamp-1 (a marker of lysosomes). At the later time-points LC3 punctate staining became negligible during a period in which the vacuoles became almost uniformly Lamp-1 positive, suggesting that all autophagosomes had fused to lysososmes (Fig. 2). Given that the autophagosomes may fuse with the endocytic compartment before fusing with lysosomes (Stromhaug and Seglen 1993) we cannot rule out the possibility that LC3, reported as a specific marker of autophagosomes (Kabeya *et al*. 2000) can also label the autophagic vacuoles formed by the fusion between autophagosome and endosomes (Liou *et al*. 1997). This possibility is presently under investigation.

Autophagy is blocked by IGF-1 and Forskolin

We and others have reported previously that hrIGF-1 and forskolin, two drugs that work on two different but correlated

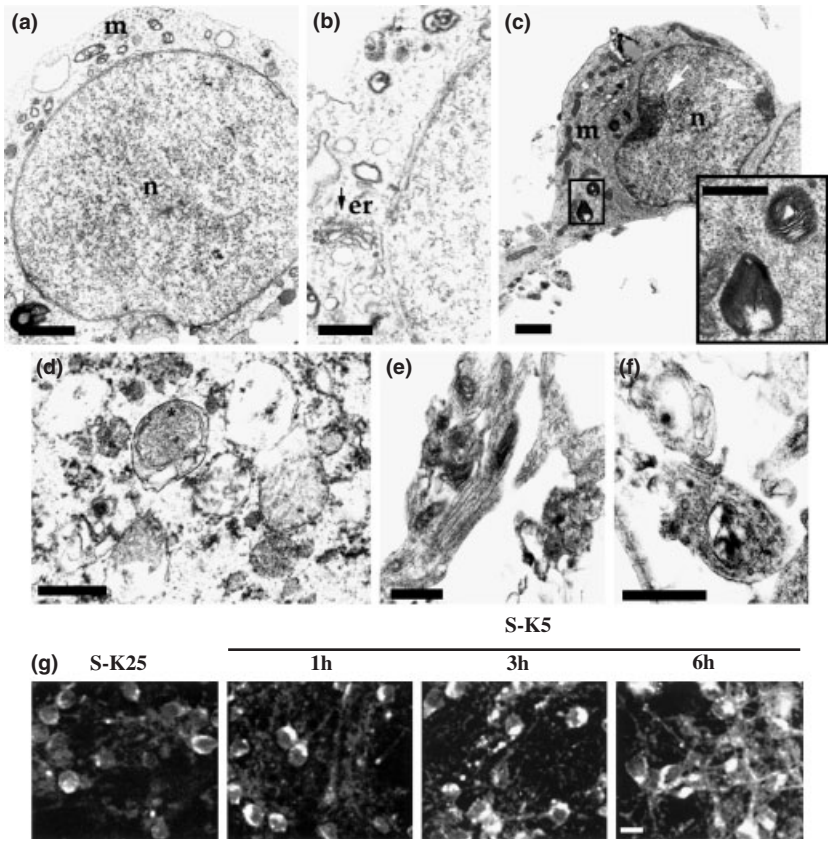

Fig. 1 Morphology of the autophagosomal/lysosomal compartment during CGCs apoptosis. CGCs were induced to undergo apoptosis for 6 h, collected and prepared for transmission electron microscopy as described in Materials and methods. (a, b) Control neurons exhibit large nuclei (n) with uniform chromatin and a small rim of cytoplasm containing a normal complement of mitochondria (m) and endoplasmic reticulum (er) (b, arrow). (c, d) Apoptotic neurons exhibit condensed mitochondria (m), chromatin packaged in electron-dense structures along the nuclear membrane (white arrows) and enhanced autophagic activity. The cytoplasm contains large electron-dense membranous whorls and vacuoles (c) engulfed of organelles such as mitochondria (d, *) at different stage of degenerative alterations. These vacuoles are also present along the neurites (e, f) in longitudinal and transversal section of neurites, respectively. (g) MDC-labelled vacuoles during progressive times of apoptosis. At the time indicated, neurons were labelled with MDC, fixed and analysed by fluorescence microscopy as described in Materials and methods. Bar: 1 μm (a and c); Bar: 0.5 μm (b, d, e, f and inset in c); Bar: 7 μm (g).

signal transduction pathways, are powerful inhibitors of CGCs apoptosis (D'Mello *et al*. 1993; Galli *et al*. 1995; Miller *et al*. 1997). As different stimuli can induce both autophagy and apoptosis *in vitro* (Isahara *et al*. 1999; Xue *et al*. 1999; Zaidi *et al*. 2001) we investigated the effect of these substances in regulating autophagosome formation in CGCs apoptosis. For this purpose immunofluorescence analysis was performed 6 h after apoptosis induction in the absence or presence of hrIGF-1 (25 ng/mL) or forskolin (10 μM). As shown in Fig. 3a, hrIGF-1 and forskolin block the autophagosome proliferation as well as cell death assessed 24 h after apoptosis induction.

Autophagy is Bcl-2 dependent and caspase-independent

It has been reported that down-regulation of Bcl-2 expression resulted both in apoptotic and autophagic cell death (Saeki *et al*. 2000; Zaidi *et al*. 2001). In order to dissect the molecular pathway leading to activation of autophagy, we investigated the effect of adenovirus-mediated overexpression of Bcl-2 on this system. For this purpose, CGCs were transducted at 4 DIV with Ad-GFP-Bcl-2 coding vector and with control Ad-βgal vector. After 48 h, neurons were induced to undergo apoptosis for 6 h and analysed by immunofluorescence with LC3 staining. In neurons overexpressing Ad-GFP-Bcl-2 and undergoing apoptosis (Fig. 3b), the proliferation of autophagosome compartment was blocked while apoptotic neurons, overxpressing control Ad-βgal, displayed a large increase in the number of autophagosomes. It must be pointed out that under these conditions Bcl-2 overexpression protects CGCs from death as documented by the number of viable cells; confirming a previous report (Watson *et al*. 1998). Furthermore, as shown in Fig. 3c, CGCs undergoing apoptosis and treated with the pan-caspase inhibitor z-VAD-fmk exhibited a similar number

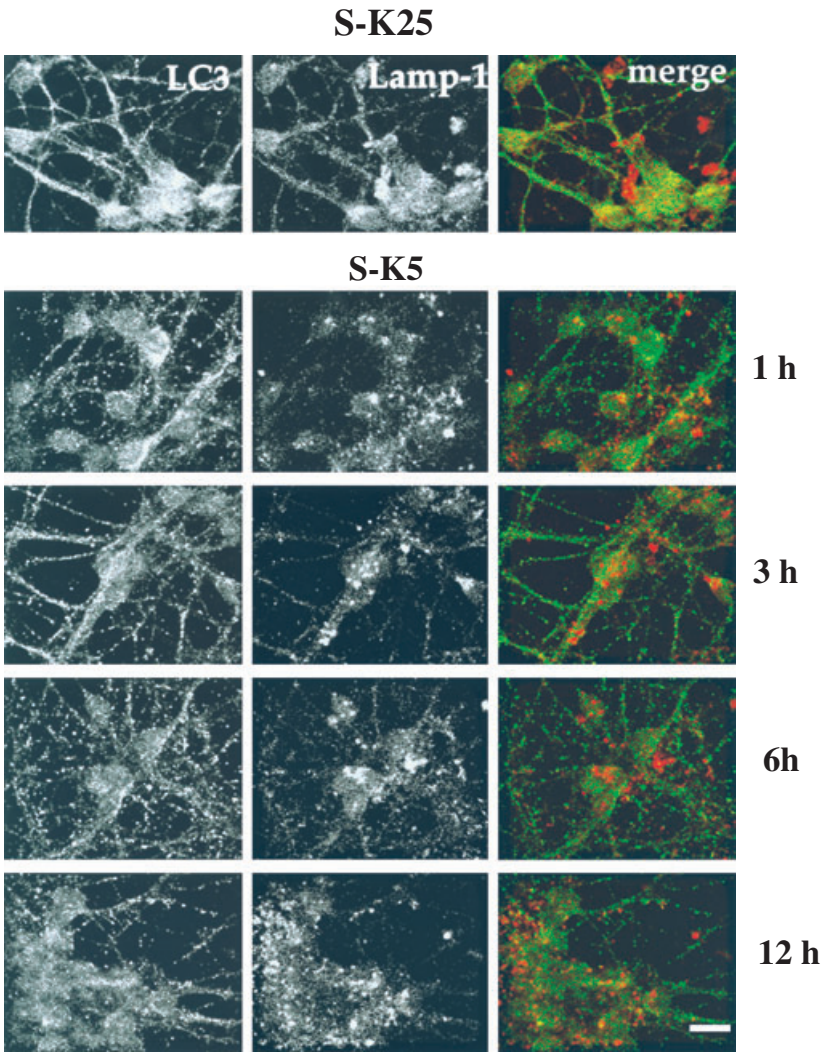

Fig. 2 Time-course of autophagic vacuole proliferation during apoptosis. CGCs were induced to undergo apoptosis for the time indicated, subjected to immunofluorescence analysis for LC3 (green) and Lamp-1 (red) and analysed by confocal microscopy. Notice that CGCs undergoing apoptosis show an LC3 punctate pattern staining, representing autophagic vacuoles, increased in number and fluorescence intensity as a function of time. Scale bar: 7 μm.

of autophagic particles as the control cells, as demonstrated by immunofluorescence analysis with the LC3 antibody. This finding indicates that inhibition of caspase does not affect autophagosome activation, and that autophagosome formation plays a caspase-independent role in the pathway leading to death of CGCs.

Inhibition of autophagy protects CGCs from cell death

To understand the role of autophagy in apoptosis, we treated CGCs undergoing apoptosis with 3-methyladenine (3-MA), a widely used, inhibitor of autophagy in mammalian cells (Seglen and Gordon 1982). This inhibitor was added to the culture medium before or at the time of apoptosis induction. Neuronal survival was determined 24 h later by the MTT assay, by counting the number of intact nuclei as described previously (Volontè *et al*. 1994; Stefanis *et al*. 1997; Stefanis *et al*. 1999) (Figs 4a and b) and by scoring the apoptotic nuclei by Hoechst 33528 staining (Fig. 4c). As reported in Figs 4a, b and C and 3-MA was a very effective inhibitor of cell death, maintaining ≈100% survival at 24 h. At later times the neuronal viability decreased to ≈80% of control. To confirm that 3-MA indeed blocked autophagy, CGCs were analysed by immunofluorescence with the anti-LC3 Ig. As shown in Fig. 4d, CGCs induced to undergo apoptosis in the presence of 3-MA showed an LC3 immunostaining pattern almost indistinguishable from that of control cells, and no LC3 positive vacuoles were observed. This finding indicates that 3-MA effectively prevents the formation of autophagosomes. We found that treatment of CGCs with either 20 or 10 mM 3-MA prevented both autophosome proliferation and cell death, without affecting neuronal morphology nor protein synthesis (data not shown). Therefore, 10 mM was the concentration chosen for the further studies.

3-MA does not promote survival by activating Akt or suppressing stress kinases activation or by stimulating purinergic receptors

In order to establish if the antiapoptotic effect of 3-MA was due to modulation of the pro-survival pathways induced by depolarization (Miller *et al*. 1997; Vaillant

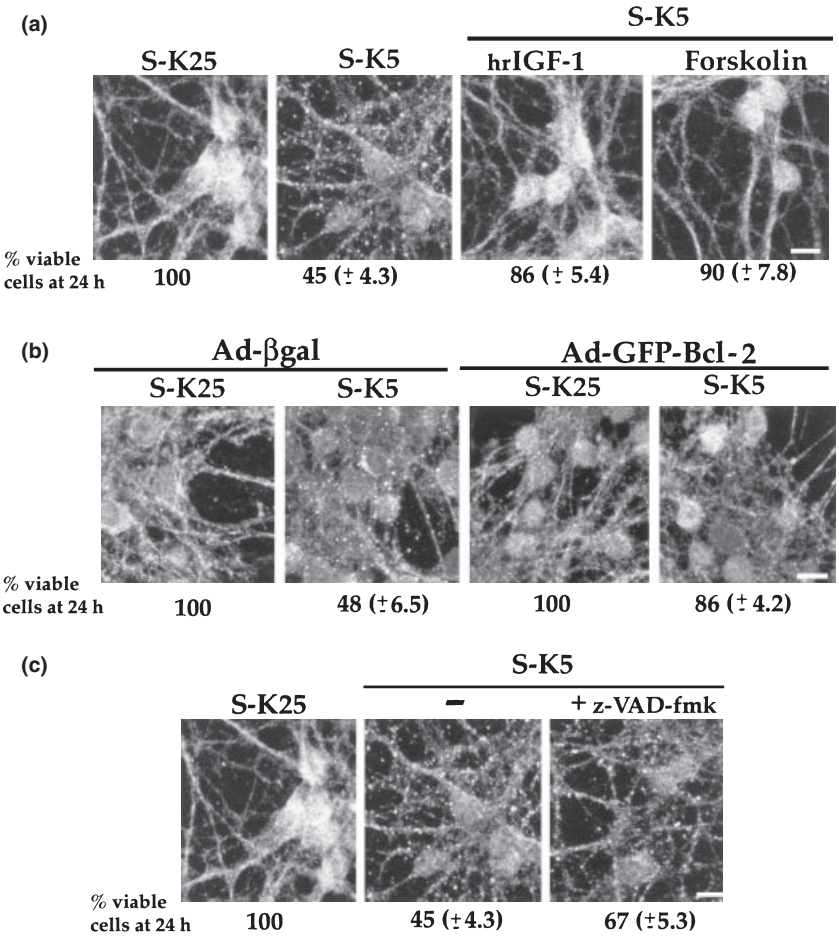

Fig. 3 Effects of antiapoptotic factors on autophagy: (a) CGCs were induced to undergo apoptosis for 6 h in the absence or in the presence of hrIGF-1 (25 ng/mL) or forskolin (10 μM) and were processed for LC3 immunostaining. Notice that hrIGF-1 and forskolin abolish the punctate immunostaining of LC3, indicating that they block its association with the membrane vacuoles. (b) CGCs were infected at 4 DIV with either β-gal or Bcl-2-expressing adenovirus vectors at MOI 30. At 6 DIV neurons were induced to undergo apoptosis for 6 h, and then analysed by scanning laser microscopy after immunostaining with anti-LC3 antibody. Notice that overexpression of Bcl-2 markedly reduces the number of LC3 positive vacuoles. (c) Immunofluorescence localization of LC3 in CGCs induced to undergo apoptosis for 6 h in the absence (S–K5) or in the presence of 100 μM z-VAD-fmk (S–K5 + z-VAD-fmk). z-VAD-fmk does not eliminate the punctate immunostaining of LC3, nor does it prevent autophagosome formation. Scale bar: 7 μm. The corresponding viability, assessed at 24 h after apoptosis induction, for the different experimental conditions is reported below each figure.

et al. 1999) or of certain stress killer kinases elicited in CGCs by potassium and serum deprivation (Watson *et al*. 1998) we investigated the effect of 3-MA on PI-3 kinase (phosphatidylinositol-3-kinase)-Akt, ERKs, p38, JNK kinases and on *p*-c-Jun. The kinase activity of Akt is sustained by phosphorylation on Ser473. This site is rapidly dephosphorylated after induction of apoptosis by potassium deprivation (Dudek *et al*. 1997; Miller *et al*. 1997). Interestingly, although the extent of phospho-Akt was markedly reduced during apoptosis, the addition of 3-MA increased this reduction (Fig. 5a) to the extent that the band was no more visible. Such a negative trend was still observed after 24 h of apoptosis (not shown). Notice that during the same period the amount of total Akt was unchanged (Fig. 5a). Akt dephosphorylation was also observed in potassium-maintained neurons treated with 3-MA (not shown). Moreover, 3-MA had a little effect on the decrease in ERK 1/2 phosphorylation seen following serum and potassium deprivation (Villalba *et al*. 1997; Harris *et al*. 2002), nor did it affect the increased phosphorylation of SAP/JNK and p38 kinases (Watson *et al*. 1998; Yamagishi *et al*. 2001; Harris *et al*. 2002) as well as of their target c-Jun occurring during apoptosis (Fig. 5a). It is worth mentioning that the state of ERK phosphorylation during apoptosis depends upon the time-schedule of apoptotic induction as when this event is triggered at 4 DIV instead than at 6 DIV, as in these experiments and in other deprivation studies, (Villalba *et al*. 1997; Harris *et al*. 2002) an increase has been reported (Subramaniam *et al*. 2003).

We have shown previously that adenosine and ADP, via interaction with A_1 and P2X receptors, respectively, markedly inhibited the program of cell death in CGCs (Vitolo *et al*. 1998). As it has been reported that adenosine and ADP are robust inhibitors of hepatocytic autophagy (Samari and Seglen 1998) we investigated whether 3-MA exerted its neuroprotective role by acting through purinergic receptors. A range of concentrations of DCPX (an A_{1A} receptor antagonist) and suramine (a non-competitive antagonist of P2X, P2Y receptors) were added to the culture medium of CGCs undergoing apoptosis in the presence or absence 3-MA, and neuronal survival was determined 24 h later. Neither DPCPX nor suramine were able to block the neuroprotective effect of 3-MA (Fig. 5b), suggesting that 3-MA does not act via purinergic receptors. Altoghether these findings suggest that 3-MA acts downstream of these apoptotic pathways.

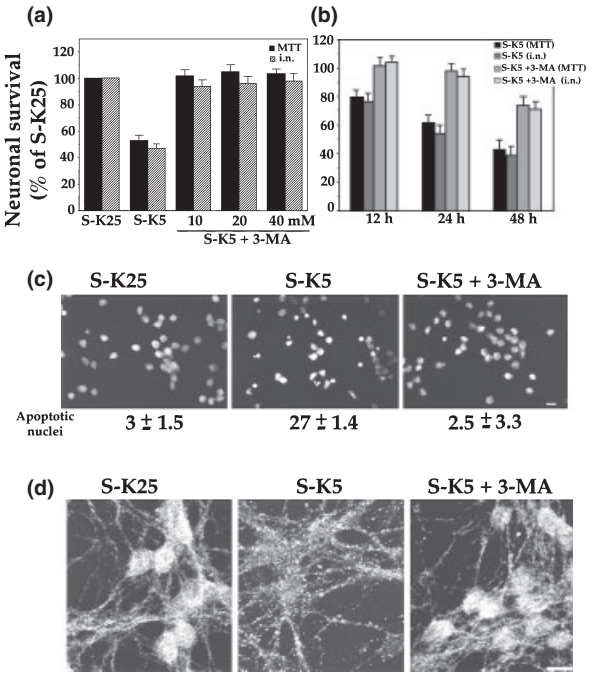

Fig. 4 3-MA blocks cell death and autophagy induced by KCl deprivation. (a) Apoptosis was induced in the absence or in the presence of different concentrations of 3-MA. After 24 h, cell viability was determined using the MTT assay or by counting the number of intact nuclei (i.n.) as described in Materials and methods. Results are the means (± SEM) of duplicate determinations from three independent experiments, and are reported as percentage of control cells. (b) Time-course of neuroprotection by 20 mM 3-MA. (c) Micrographs of Hoechst 33258-stained cultures upon 24 h of apoptosis in the absence or presence of 10 mM 3-MA. Values corresponding to apoptotic nuclei as percentages of total nuclei are reported below. (d) Autophagy was assessed by confocal microscopy 6 h after apoptosis induction. Note that apoptotic CGCs treated with 3-MA (10 mM) have a normal diffuse LC3 immunostaining, similar to that of control untreated neurons.

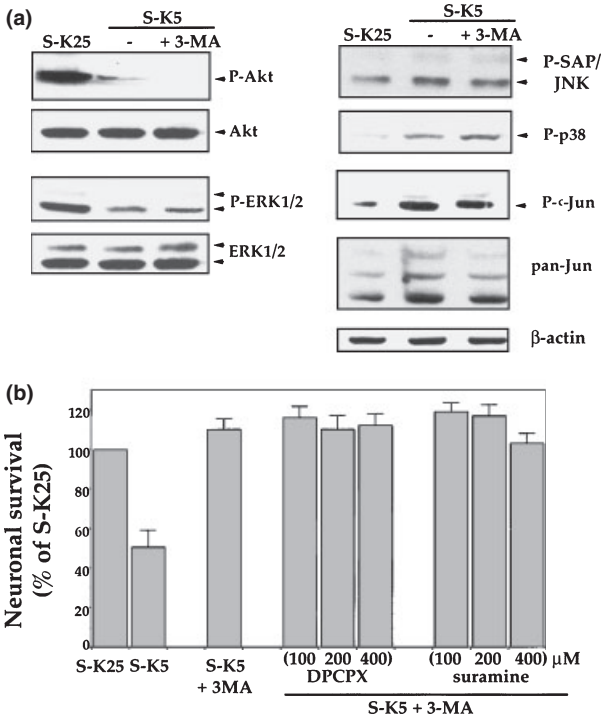

Fig. 5 The neuroprotective effect of 3-MA does not involve signalling via Akt or stress kinases or via purinergic receptors. (a) Apoptosis was induced for 6 h in the presence of 3-MA (10 mM) (S–K5 + 3-MA). Neurons were lysed and analysed by immunoblot for phospho-Akt (*p*-Akt), phospho-ERK1/2 (*p*-ERK) and for the total amount of both enzymes (a, left panel). *p*-SAP/JNK, phospho-p38 (*p*-p38), phospho-c-Jun (*p*-c-jun) and pan-Jun were labelled with specific antibodies (a, right panel). Amounts of loaded proteins were controlled for homogenity by probing the membrane with an anti-β-actin mAb. Results show a representative experiment that was repeated three times. (b) CGCs were induced to undergo apoptosis for 24 h in the absence or in the presence of 3-MA (10 mM) plus different amounts of DPCPX and suramine. Neuronal survival was determined using an MTT assay. Results are means (± SEM) of duplicate determinations from three independent experiments and are reported as percentage of control cells (S–K25 for 24 h).

3-MA inhibits morphological and biochemical features of apoptosis

To ascertain whether the neuroprotective effect of 3-MA was correlated with the inhibition of known hallmarks of serum and KCl deprivation-induced apoptosis, we assessed the extent of DNA laddering, reactive oxygen species (ROS) production and caspase activation (Schulz *et al.* 1996). Figure 6a shows that DNA cleavage induced in CGCs by serum and KCl deprivation, measured by an ELISA measuring internucleosomal DNA fragmentation assay, was completely abolished by 3-MA treatment of apoptotic CGCs.

ROS have been implicated as important effector molecules in apoptotic cell death (Hockenbery *et al.* 1993; Kane *et al.* 1993) and are reported to be released in large amount from CGCs (Atlante *et al.* 2003). ROS production was evaluated with the oxidation-sensitive indicators DCF-H2, a lipophilic non-fluorescent indicator that is oxidized by ROS to the fluorescent dye DCF. As shown in Fig. 6b, the indicator detected a peak in DCF fluorescence at 4 h after apoptosis, whose appearance was largely blocked in cells treated with 3-MA.

DNA fragmentation and ROS production occur downstream of caspase activation (Schulz *et al.* 1996). Among caspases, caspase-3 is a key component of CGC's apoptosis (Eldadah *et al.* 1997; Canu *et al.* 2000). Therefore, we examined the possible involvement of 3-MA in the regulation of caspase-3 activity. As shown in Fig. 6c, caspase-3 like activity was approximately 10-fold elevated in apoptotic neurons with respect to control (S–K25) neurons. In contrast, neurons treated with 3-MA and subjected to apoptotic stimuli exhibited an almost undetectable activation. Moreover, addition of 10 or 20 mM 3-MA to apoptotic cell lysate did not reduce caspase-activity, indicating that 3-MA operates by blocking caspase activation rather than caspase-3 activity.

This conclusion was further supported by assessing the effect of 3-MA on pro-caspase-3 processing. By exploiting an antiserum that specifically recognizes the cleaved, active form of caspase-3, we found that neurons induced to undergo apoptosis were strongly immunostained (Fig. 6d, arrows) whereas neurons treated with 3-MA were barely immunolabelled, consistent with the conclusion that pro-caspase-3 protein remained uncleaved.

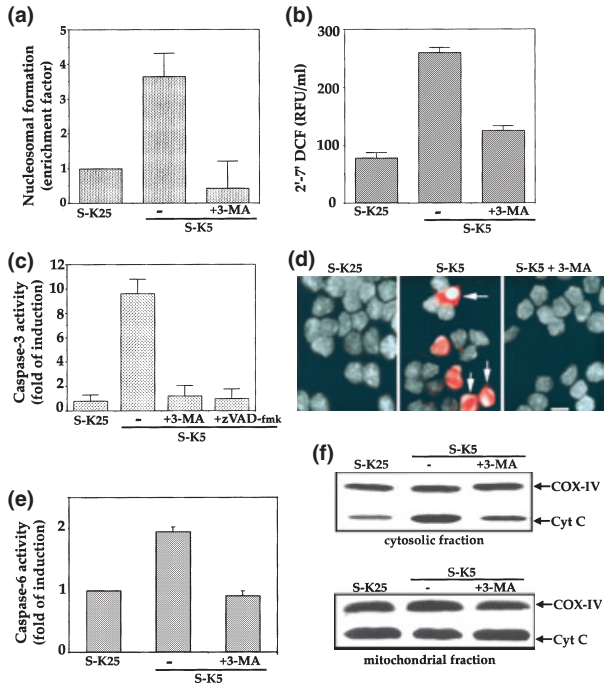

Fig. 6 3-MA inhibits the appearance of apoptotic markers. (a) CGCs were induced to undergo apoptosis for 10 h in the absence or in the presence of 3-MA (10 mM), and DNA fragmentation was measured as described in Material and methods. Data are the mean (± SEM) (n = 3). (b) 10 mM 3-MA inhibits ROS production detected by dihydrorhodamine 123 fluorescence measured 4 h after apoptosis. Results are reported as the mean (± SEM) (n = 4). (c) Eight hours after apoptosis in the presence or absence of 3-MA (10 mM) neurons were lysed and assayed for DEVD-MCA cleavage. (d) CGCs were immunostained with an antibody against cleaved caspase-3 (Asp175) (red) and counterstained with the DNA dye Hoechst for nuclei (white). Notice that 3-MA fully inhibits caspase-3 activity (c) and activation (d) into the cytoplasm of apototic neurons (arrows indicate change in caspase-3 positive neurons). Scale bar: 7 μm. (e) Caspase-6 activity was measured 1 h after apoptosis using the fluorogenic substrate VEID-MCA. Fold-induction of caspase-3 and caspase-6 activities are the means (± SEM) of triplicate determinations from three independent experiments. (f) Western blot analysis of cyt *c*. Either cytosolic or respective mitochondrial fraction from CGCs, induced to undergo apoptosis for 3 h in the absence or in the presence of 3-MA (10 mM), were analysed by Western blotting analysis. An antibody against mitochondrial COX-IV was used as a marker of mitochondrial contamination of cytosolic extracts and as control of protein loading/transfer.

Inhibition of caspase-6 activity by CP-VEID-cho, prevents caspase-3 activation in granule neurons undergoing apoptosis (Allsopp *et al*. 2000), and we therefore investigated its activity in 3-MA treated neurons. As reported in Fig. 6e, caspase-6 activity in neurons treated with 3-MA was identical to that of control cells, while apoptotic neurons displayed an approximately twofold increase 1 h after the onset of apoptosis (Allsopp *et al*. 2000). Taken together, these studies strongly suggest that inhibition of autophagic activity suppresses the pathway leading to the activation of caspase-3-like proteases rather than directly inhibiting these enzymes.

3-MA prevents cytochrome *c* release

The intrinsic (mitochondrial) death pathway plays through the release of mitochondrial cytochrome *c* (cyt *c*), an important role in CGCs apoptosis (Bobba *et al*. 1999). To determine whether inhibition of autophagosome formation prevented the intrinsic apoptotic pathway, the release of cyt *c* was investigated by Western blotting analysis of cytosolic and mitochondrial fraction. As shown in Fig. 6f, cyt *c* was released in the cytosol of CGCs induced to undergo apoptosis for 3 h as reported previously by Bobba *et al*. (1999). Addition of 3-MA during apoptosis markedly diminished the release of cyt *c* from mitochondria to cytosol. Thus, 3-MA inhibits the release of cyt *c* from mitochondria and the subsequent activation of caspases.

The autophagosomal/lysosomal compartment controls caspase-3 activation through cathepsin B

3-MA stops macro-autophagy at the sequestration step in mammalian cells (Seglen and Gordon 1982), so we asked whether inhibition at different steps would prevent cell death and/or relieve specific apoptotic features such caspase activation.

Inhibitors of autophagy acting downstream of the sequestration phase, such as bafilomycin A(1), a specific inhibitor of vacuolar H (+)-ATPase, and inhibitors of the cathepsin D and L (pepstatin and z-FA fmk) were not able to block the death process at 24 h (Fig. 7a) nor did they suppress caspase activity (Fig. 7c). In contrast, CA074-Me, a selective inhibitor of cathepsin B (Buttle *et al*. 1992) was able to delay cell death and to interfere with caspase activation (Fig. 7b). In the presence of this drug neurons remained alive for 12–15 h. At later time points, the neuroprotective effect was less evident (Fig. 7a) and at longer time points it was not more detectable (not shown), probably because in the presence of this compound autophagic activity remains elevated (Fig. 7b). Nevertheless, inhibitors of cathepsin B were able to prevent caspase-3 activation. Z-FA-fmk and CA074-Me did not appear to inhibit the activity of preactivated caspase-3 as addition of these compounds to lysates of apoptotic CGCs, at the time of substrate addition, did not inhibit DEVD-MCA hydrolysis (Fig. 7C). Instead, they appear to act by inhibiting caspase

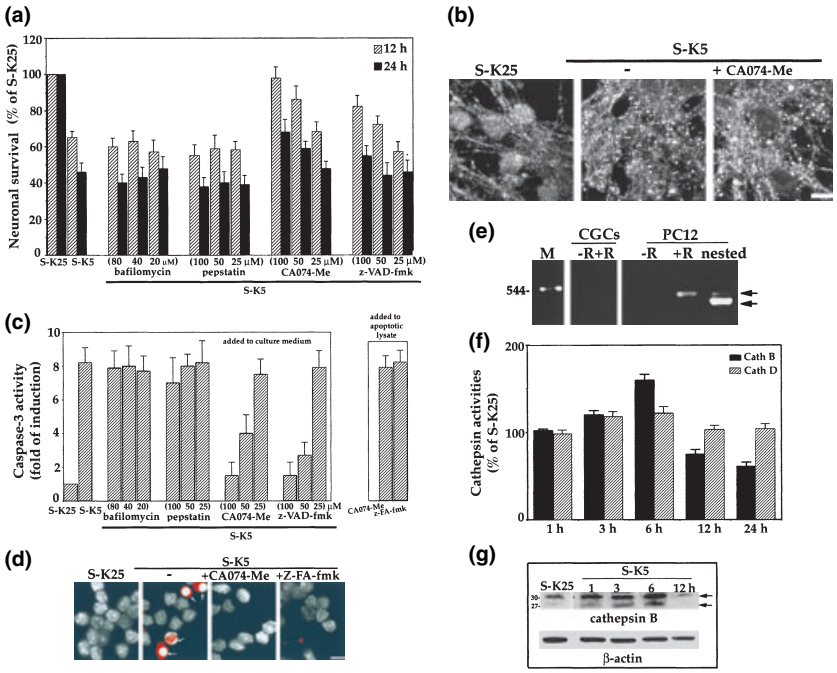

Fig. 7 Inhibitors of cathepsin B delay cell death and prevent caspase-activation. CGCs, were induced to undergo apoptosis in the absence or in the presence of different concentration of bafilomycin, an inhibitor of the vacuolar ATPase proton pump; pepstatin, an inhibitor of cathepsin D; z-FA -fmk, an inhibitor of cathepsin B and L; and CA074-Me a selective inhibitor of cathepsin B. (a) Neuronal survival was determined 12 and 24 h after apoptosis by counting the number of intact nuclei. Similar results were obtained by MTT assay. Survival is reported as percentage of control cells (S–K25) and is the mean ± SEM ($n = 3$). (b) CGCs were induced to undergo apoptosis for 6 h in the absence or in the presence of CA074-Me and were processed for LC3 immunostaining. Notice that CA074-Me does not abolish the punctate immunostaining of LC3, indicating that it does not prevent autophagy. (c) Caspase-3 activity was determined 8 h after apoptosis induction in the presence of the same substances and expressed as fold of induction with respect to controls (S–K25) neurons. The activity is expressed in arbitrary units. Data is the mean ± SEM ($n = 3$). (d) Six hours after apoptosis induction, neurons were immunostained with an antibody against cleaved caspase-3 (Asp175; red) and counterstained with the DNA dye Hoechst for nuclei (white). Notice the complete inhibition of pro-caspase-3 activation exerted by CA074-Me and z-FA-fmk detectable in apoptotic neurons and evidenced by arrows. (e) Seven DIV neurons were washed twice with S–K25 medium and total RNA was isolated. After reverse transcription (+ R) and PCR amplification for cathepsin E, DNA was electrophoresed and visualized with ethidium bromide. Reverse transcriptase was omitted in control experiments (– R). The predicted fragment size was of 383 bp and 325 bp in the nested PCR. PC12 cells were utilized as a positive control for cathepsin E expression. (f) Cathepsin D and cathepsin B activities in cell lysates of CGCs obtained at 1, 3, 6, 12 and 24 h after the induction of apoptosis (S–K5). For each time point the activities of cathepsin D and B are reported relative to controls (S–K25). The values represent means of a triplicate determination (± SD) from three independent experiments. (g) Expression of cathepsin B during CGCs apoptosis. After 1, 3, 6, 12, and 24 h of apoptosis, 25 μg of total cellular proteins were analysed by Western blot using a rabbit antibody against cathepsin B. Immureactivity for β-actin band is shown to demonstrate the uniformity of protein loading/transfer.

activation. This latter conclusion was further corroborated by finding that both z-FA-fmk and CA074-Me were able to prevent pro-caspase 3 activation, as shown by immunofluorescence analysis performed with an antibody that specifically recognized cleaved caspase-3 (Asp175) (Fig. 7d).

We next determined the proteolytic activity of lysosomal cathepsin D and B. Cathepsin D was measured by incubating the cell lysates with the fluorogenic substrate MOAc-Gly-Lys-Pro-Ile-Leu-Phe-Phe-Arg-Leu-Lys (Dnp)g-NH2. This substrate is hydrolysed equally by cathpesin D and E (Yasuda *et al.* 1999). It has been reported that cathepsin E is barely, if at all, expressed in cerebellum (Yasuda *et al.* 1999) and we similarly failed to detect cathepsin E mRNA in CGCs by RT-PCR (Fig. 7e). Therefore, the enzymatic activity tested in these lysates by this assay is likely to reflect cathepsin D alone. Cathepsin B activity was measured by incubating the cell lysates with the cathepsin B specific substrate Z-Arg-Arg-MCA (Barret and Kirschke 1981).

While the activity of cathepsin D was only slightly modulated during the progression of apoptosis, that of cathepsin B rapidly increased reaching ≈150% of its initial activity 6 h after the onset of apoptosis, when it drastically declined to ≈80% of its initial activity at 24 h (Fig. 7f). Cathepsin B is synthesized as a proenzyme and is transported into lysosomes where it is processed into active

forms, a two-chain form (25–27 kDa) and a single-chain form (29–31 kDa). As can been seen in Fig. 7g, the amount of the precursor and the mature forms of cathepsin B increased in the first 6 h of apoptosis, and declined thereafter.

Cathepsin B is relocated from lysosomes to the cytoplasm during apoptosis

The finding that inhibition of cathepsin B blocked caspase-3 activation, raised the question of how an enzyme normally confined to the endolysosomal compartment could be involved in the activation of the caspase cascade that, to date, is reported to take place in the cytosol. One possibility is that cathepsin B translocates into the cytosol during apoptosis, as also reported in other *in vitro* models of apoptosis (Guicciardi *et al*. 2000).

In order to assess this hypothesis, we used immunofluorescence and Western blot analysis to visualize the cellular distribution of cathepsin B in CGCs. As shown in Fig. 8a, cathepsin B exhibited a pronounced punctate staining in

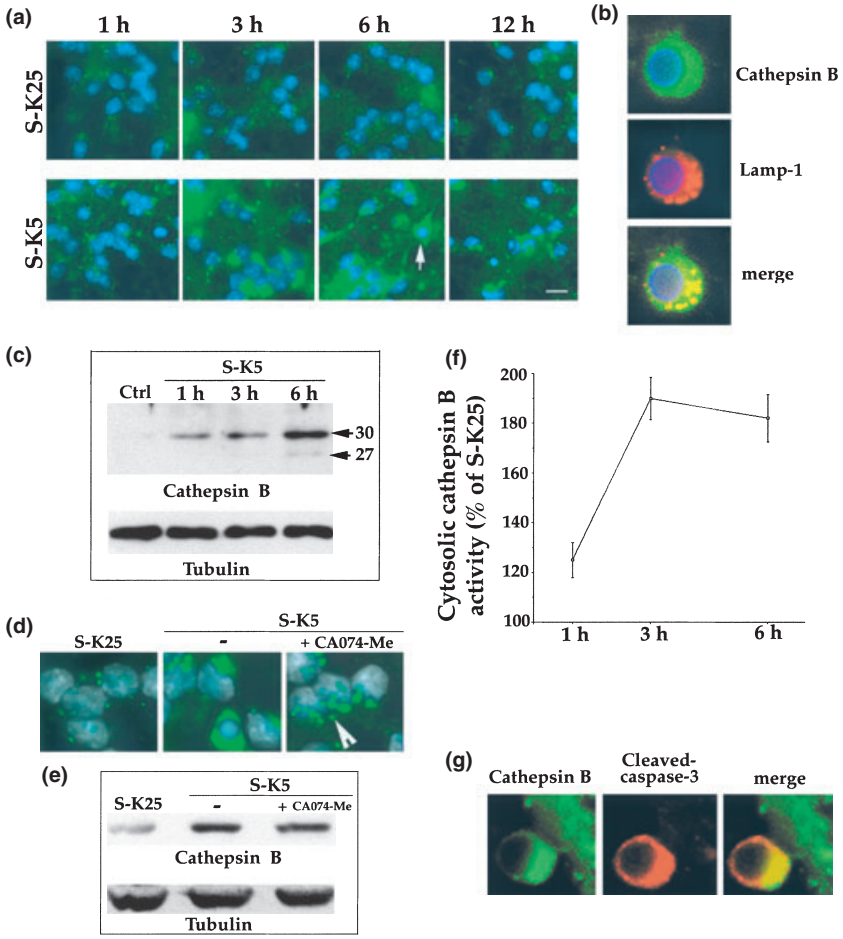

Fig. 8 Cathepsin B is translocated in the cytosol during CGCs apoptosis. (a) CGCs were induced to undergo apoptosis for the time indicated, stained by immunofluorescence analysis for cathepsin B (green) and analysed by confocal microscopy. Nuclei were stained with Hoechst (blue). (b) Cathepsin B is spread into the cytoplasm (green) of apoptotic neurons [stained with Hoechst (blue)] while lysosome membranes stained with lamp-1 (red) appear intact as also evidenced by merge analysis. (c) Cytosolic extracts from CGCs undergoing apoptosis were prepared at indicated times and subjected to Western blot analysis with a rabbit anti-cathepsin B antiserum. Amounts of loaded proteins were controlled for homogenity by probing membrane with anti-α-tubulin. Results are from one of two representative experiments. (d, e) Release of cathepsin B in the cytosol is not prevented by CA074-Me. (d) Immunoflourecence analysis for cathepsin B (green) in CGCs undergoing apotosis in the absence (–) or presence (+) of CA074-Me. Notice the persistence of a diffuse staining of cathepsin B (white arrow) in CGCs treated with CA074-Me. (e) Cytosolic extracts from CGCs undergoing apoptosis, in the absence (–) or in the presence (+) CA074-Me were prepared at 3 h of apoptosis and subjected to Western blot analysis with rabbit anti-cathepsin B antiserum. Amounts of loaded proteins were controlled for homogenity by probing membrane with anti-α-tubulin. Results are from one of two representative experiments. (f) Equal amounts of cytosolic proteins were analysed for cathepsin B activity using the fluorogenic protease substrate z-RR-MCA. Results are means ± SEM from a triplicate experiment and are referred to control values. (g) Colocalization of cytosolic cathepsin B (green) and activacted pro-caspase-3 (red) in an apoptotic neuron. Bar: 7 μm.

control cells, consistent with its lysosomal localization. After induction of apoptosis, an increase in cathepsin B immunostaning was observed, in agreement with data reported in Fig. 7f, and the staining became diffusely distributed in the cytoplasm of apoptotic neurons, recognizable as those having Hoechst-positive nuclei (Fig. 8a, arrow). It is noteworthy that co-immunostaining of the lysosomes with mAb against Lamp-1 showed a punctate immunolabelling that did not disappear during apoptosis, indicating that the lysosomal membranes were still preserved when cathepsin B is present in the cytosol (Fig. 8b). Further evidence of translocation of cathepsin B is indicated by immunoblot analysis showing that the cathepsin B active fragments (p30 and p27) increased in the cytosol of CGCs induced to undergo apoptosis (Fig. 8c). Thus, these results are consistent with a translocation from a vesicular compartment into the cytosol, or to an altered trafficking of cathepsin B during apoptosis. We found that, when CGCs were induced to undergo apoptosis in the presence of the cathepsin B inhibitor CA074-Me, cathespin B translocation was not prevented (Figs 8d and e), suggesting that the loss of lysosome membrane integrity or function is not cathepsin B-dependent. Similar results were also obtained when CGCs were treated with lipid peroxidation inhibitors (data not shown).

We next addressed the question of whether cathepsin B was active in the cytosol of apoptotic neurons. As shown in Fig. 8d, cytosolic cathepsin B activity was detected as soon as 3 h after KCl withdrawal and reached a maximum at 6 h when it started to decline (Fig. 8f). Given the emerging role of cathepsin B in regulating caspase-3 activation and activity, we performed a double-immunostaining for both proteins and we found that cathepsin B and activated pro-caspase-3 colocalized in the cytosol of apoptotic neurons (Fig. 8g). This finding further underlines the potential significance of cathepsin B translocation in caspase activation.

Discussion

In the present work we provide evidence for the activation of an autophagic process within the context of the apoptotic program of CGCs. In particular, we have established a causal role of autophagosomal/lysosomal compartment, via cathepsin B, in the activation of the caspase-cascade and provide evidence that autophagy may mediate a program of caspase-independent cell death.

Cultured CGCs deprived of depolarizing concentrations of potassium are one of the most widely employed model for the investigation of neuronal apoptosis. Although it has been reported previously that this manipulation causes classical apoptotic cell death (D'Mello *et al*. 1993), the data presented in this paper suggest that the situation is more complex and that this type of death is geared with autophagy.

Activation of the autophagosome/lysosomal compartments, monitored by electron microscopy, MDC labelling and LC3 and Lamp-1 immunostaining (Figs 1 and 2) occurs very early after induction of apoptosis, before the classical apoptosis morphology is manifested (Fig. 2). These degradative compartments expanded with time, and were most abundant in cells that also contained fragmented or pycnotic nuclei. Several findings suggest that the existence of two populations of cells (undergoing apoptotic and autophagic death, respectively) is unlikely. Thus, it is worth noting that autophagosomes were more abundant in cells with the earliest nuclear and cytoplasmic alteration of apoptosis (Fig. 1c). Moreover, the full protection exterted by the anti-autophagic 3-MA points to an homogeneous population (Figs 3 and 6). Therefore, we favour the hypothesis, presently under investigation, that there is a transition within each cell from autophagic to an apoptotic process.

While the mechanism of autophagy induction in CGCs remains to be established we found that it is was fully prevented by hrIGF-1 and forskolin and by overexpression of Bcl-2. It has been reported stimulation of class I PI-3 kinase activity inhibits, whereas class III PI-3 kinases induce, autophagic sequestration (Petiot *et al*. 2000). As far as IGF-1 is concerned, it is probable that it inhibits autophagy by regulating the phosphorylation state of the PI-3-kinases of class I. Forskolin acts by increasing the intracellular concentration of cAMP, whose role in inhibiting the sequestration phase of autophagy has been reported (Holen *et al*. 1996).

Members of the Bcl-2 family play an important role in programmed cell death in the developing brain (Kuan *et al*. 2000). Recent data also supported an involvement of these factors in autophagic cell death. In fact, Bcl-XL deficiency induced, and Bax deficiency inhibited, chloroquine-induced cell death of cortical neurons (Zaidi *et al*. 2001). Moreover, antisense-mediated down regulation of Bcl-2 in leukaemia cells caused an extensive autophagic cell death (Saeki *et al*. 2000). Our data are in line with these studies, as overexpression of Bcl-2 largely inhibited the proliferation of the autophasomal compartment and protected CGCs from death. How this effect is achieved remains to be elucidated. It is possible that the interaction of Bcl-2 with beclin-1 is involved. Beclin-1, the mammalian homologue of yeast *Apg6* gene, induces autophagy (Liang *et al*. 2001) complexing with the *trans*-Golgi network (Kihara *et al*. 2001). During CGCs apoptosis a functional depletion of Bcl-2 occurs, due to down-regulation of antiapoptotic Bcl-2 proteins (Alavez *et al*. 2003) and, in particular, to up-regulation and mislocalization of proapoptotic Bcl-2 proteins (Harris and Johnson 2001; Putcha *et al*. 2002). Therefore, it is tempting to speculate that beclin-1 could be released from the Bcl-2/beclin-1 complex thus activating autophagy by interacting with PI3-kinase. However, further investigations are required to explore this hypothesis.

Our study demonstrates that, in this model of neuronal death, induction of autophagy is caspase-independent. In fact, caspase-3 activation occurs downstream of, and appears to depend upon, induction of autophagy. Thus, we found that 3-MA was able to protect caspase-inhibited neurons from delayed cell death (data not shown). This observation suggests that, once activated, autophagy actively contributes to channel CGCs to death. Previous studies have attributed a critical role in apoptosis to autophagy; a process triggered by NGF deprivation in sympathetic neurons (Xue *et al*. 1999); serum deprivation in PC12 cells (Isahara *et al*. 1999); chloroquine in cortical neurons (Zaidi *et al*. 2001) and by brief ischemia in CA1 pyramidal neurons in the gerbil hyppocampus (Nitatori *et al*. 1995), by *N*-methyl-D-aspartate in organotypic hippocampal cultures (Borsello *et al*. 2003) or by tamoxifen in human mammary carcinoma cells (Bursch 2001).

Likewise, inhibition of autophagy in CGCs by 3-MA, prevented both cell death and autophagosome proliferation.

3-MA did not induce activation of Akt indicating that this pathway does not contribute to CGC protection. Moreover, the neuroprotective effect of 3-MA did not involve the supression of JNK pathway (Harris *et al*. 2002) nor the activation of purinergic receptors, previously reported to exert a neuroprotective effect against apoptosis (Vitolo *et al*. 1998). Altogether these findings suggest that the steps inhibited by 3-MA lie further downstream. Given the role of Bcl-2 in suppressing autophagy, it is tempting to speculate that 3-MA may act on the same steps that are postulated to initiate autophagy likely at the level of PI-3 kinase/Bcl-2 complex. Thus, 3-MA leads to inhibition of the release of cytochrome *c* from mitochondria into the cytosol, therefore preventing activation of the active form of caspase 3 (Fig. 6a and b), and of other caspases.

To better understand the role of autophagy in the activation of caspases, we pharmacologically inhibited the autophagy downstream of the sequestration phase. We found that, only inhibitors of cathepsin B were able prevent caspase-activation and to exert a transitory vital role (Figs 7a, c and d). It is probable that the lack of long-terminal survival is due to the persistence of autophagic activity in CGCs treated with cathepsin inhibitor (Fig. 7b). This situation mimicks that of caspase-inhibited CGCs (Fig. 6c).

Cathepsins have been implicated in a number of important cellular processes such as protein degradation, antigen presentation and cell death. We showed, that the activation and translocation of cathepsin B was a crucial event in CGCs undergoing apoptosis, as reported recently for TNF-triggered apoptosis (Foghsgaard *et al*. 2000; Guicciardi *et al*. 2000), and for TWEAK-induced cell death (Nakayama *et al*. 2002). The finding that translocation of cathepsin B was not prevented by cathepsin B inhibitor (Fig. 8) nor by inhibitors of lipid peroxidation (not shown) suggests that other factors are responsable for the lack of lysosomal membrane integrity.

Given that autophagy requires the dynamic mobilization of cellular membranes and specialized protein machinery we can not rule out the possibility that an altered sorting of lysosome enzymes may occur during apoptosis. Whatever the mechanism that underlies cathepsin B translocation, the finding that CGCs were protected by the cathepsin B inhibitor CA074-Me, even though cathepsin B was still translocated to the cytosol, indicates that this process is not necessarily detrimental to cell viability, per se. The importance of cathepsin B has been demonstrated previously in studies of animals deficient in the endogenous cathepsin B inhibitor, cystatin B, which suffer a drastic loss of CGCs by apoptosis (Houseweart *et al*. 2003). In our *in vitro* experiments, it is possible that cystatin activity is lost, therefore allowing cathepsin B to initiate and propagate the execution phase of apoptosis. It remains to be investigated whether this phase involves cathespin B-mediated release of cyt *c* in the mitochondrial death pathway or, alternatively, proceeds via direct or indirect activation of caspase, as suggested recently (Stoka *et al*. 2001).

Acknowledgements

This study was supported in part by Ministero della Sanità Grant ICS 110.1/RA00.54 to NC, Progetto Strategico sulla Malattia di Alzheimer del Ministero della Sanità and FIRB-PNR to PC.

We thank Dr T. Yoshimori for supplying us the LC3 antibodies, Dr J. Mort for rat cathepsin B antibodies and Dr M. Crescenzi for Ad-Bcl-2 and Ad-βgal vectors vector. We thank Dr Tiziana Parassassi for her help in spectroflurimetric determination of cathepsin activities. We thank Prof. A. Turkewitz for comments on this manuscript.

References

Alavez S., Pedroza D. and Moran J. (2003) Mechanisms of cell death by deprivation of depolarizing conditions during cerebellar granule neurons maturation. *Neurochem. Int.* **43**, 581–590.

Allsopp T. E., McLuckie J., Kerr L. E., Macleod M., Sharkey J. and Kelly J. S. (2000) Caspase 6 activity initiates caspase 3 activation in cerebellar granule cell apoptosis. *Cell Death Differ.* **7**, 984–993.

Amadoro G., Serafino A. L., Barbato C., Ciotti M. T., Sacco A., Calissano P. and Canu N. (2004) Role of N-terminal tau domain integrity on the survival of cerebellar granule neurons. *Cell Death Differ.* **11**, 217–230.

Atlante A., Bobba A., Calissano P., Passarella S. and Marra E. (2003) The apoptosis/necrosis transition in cerebellar granule cells depends on the mutual relationship of the antioxidant and the proteolytic systems which regulate ROS production and cytochrome c release en route to death. *J. Neurochem.* **84**, 960–971.

Barret A. J. and Kirschke H. (1981) Cathepsin B, cathepsin H. & cathepsin L. *Methods Enzymol.* **80**, 535–561.

Biederbick A., Kern H. F. and Elsasser H. P. (1995) Monodansylcadaverine (MDC) is a specific *in vivo* marker for autophagic vacuoles. *Eur J. Cell Biol.* **66**, 3–14.

Bobba A., Atlante A., Giannattasio S., Sgaramella G., Calissano P. and Marra E. (1999) Early release and subsequent caspase-mediated

degradation of cytochrome c in apoptotic cerebellar granule cells. *FEBS Lett.* **457**, 126–130.

Borsello T., Croquelois K., Hornung J. P. and Clarke P. G. H. (2003) N-methyl-D-aspartate triggered neuronal death in organotypic hippocampal cultures is endocytic, autophagic and mediated by the c-jun N-terminal kinase pathway. *Eur. J. Neurosci.* **18**, 473–485.

Bursch W. (2001) The autophagosomal-lysosomal compartment in programmed cell death. *Cell Death Differ.* **8**, 569–581.

Buttle D. J., Murata M., Knight C. G. and Barret A. J. (1992) CA074 methyl ester: a proinhibitor for intracellular cathepsin B. *Arch. Biochem. Biophys.* **299**, 377.

Canu N., Barbato C., Ciotti M. T., Serafino A., Dus L. and Calissano P. (2000) Proteasome involvement and accumulation of ubiquitinated proteins in cerebellar granule neurons undergoing apoptosis. *J. Neurosci.* **20**, 589–599.

Clarke P. G. (1990) Developmental cell death: morphological diversity and multiple mechanisms. *Anat. Embryol.* **181**, 195–213.

D'Mello S. R., Galli C., Ciotti T. and Calissano P. (1993) Induction of apoptosis in cerebellar granule neurons by low potassium: inhibition of death by insulin-like growth factor I and cAMP. *Proc. Natl Acad. Sci. USA* **90**, 10 989–10 993.

Deiss L. P., Galinka H., Berissi H., Cohen O. and Kimchi A. (1996) Cathepsin D protease mediates programmed cell death induced by interferon-gamma, Fas/APO-1 and TNF-alpha. *EMBO J.* **15**, 3861–3870.

Dudek H., Datta S. R., Franke T. F., Birnbaum M. J., Yao R., Cooper G. M., Segal R. A., Kaplan D. R. and Greenberg M. E. (1997) Regulation of neuronal survival by the serine-threonine protein kinase Akt. *Science* **275**, 661–665.

Eldadah B. A., Yakovlev A. G. and Faden A. I. (1997) The role of CED-3-related cysteine proteases in apoptosis of cerebellar granule neurons. *J. Neurosci.* **17**, 6105–6113.

Foghsgaard L., Wissing D., Mauch D., Lademann U., Bastholm L., Boes M., Elling F., Leist M. and Jaattela M. (2000) Cathepsin B acts as a dominant execution protease in tumor cell apoptosis induced by tumor necrosis factor. *J. Cell Biol.* **153**, 999–1010.

Galli C., Meucci O., Scorziello A., Werge T. M., Calissano P. and Schettini G. (1995) Apoptosis in cerebellar granule neurons is blocked by high KCl, forskolin, and IGF-1 through distinct mechanisms of action. the involvement of intracellular calcium and RNA synthesis. *J. Neurosci.* **15**, 1172–1179.

Gallo V., Balazs R. and Jorgensen O. S. (1985) Cell surface proteins of cerebellar interneurones and astrocytes cultured in chemically defined and serum-supplemented media. *Brain Res.* **349**, 27–37.

Guicciardi M. E., Deussing J., Miyoshi H., Bronk S. F., Svingen P. A., Peters C., Kaufmann S. H. and Gores G. J. (2000) Cathepsin B contributes to TNF-alpha-mediated hepatocyte apoptosis by promoting mitochondrial release of cytochrome c. *J. Clin. Invest.* **106**, 1127–1137.

Guimaraes C. A., Benchimo M., Amarante-Mendes G. P. and Linden R. (2003) Alternative programs of cell death in developing retinal tissue. *J. Biol. Chem.* **278**, 41 938–41 946.

Hacker G. (2000) The morphology of apoptosis. *Cell Tissue Res.* **301**, 5–17.

Harris C. and Johnson E. M. Jr (2001) BH3-only Bcl-2 Family members are coordinately regulated by the JNK pathway and require bax to induce apoptosis in neurons. *J. Biol. Chem.* **276**, 37 754–37 760.

Harris C., Maroney A. C. and Johnson E. M. Jr (2002) Identification of JNK-dependent and -independent components of cerebellar granule neuron apoptosis. *J. Neurochem.* **83**, 992–1001.

Hengartner M. O. (2000) The biochemistry of apoptosis. *Nature* **407**, 770–776.

Hockenbery D. M., Oltvai Z. N., Yin X.-M., Milliman C. L. and Korsmeyer S. J. (1993) Bcl-2 functions in an antioxidant pathway to prevent apoptosis. *Cell* **75**, 241–251.

Holen I., Gordon P. B., Stromhaug P. E. and Seglen P. O. (1996) Role of cAMP in the regulation of hepatocytic autophagy. *Eur J. Biochem.* **236**, 163–170.

Houseweart M. K., Pennacchio L. A., Vilaythong A., Peters C., Noebels J. L. and Myers R. M. (2003) Cathepsin B but not cathepsins L or S contributes to the pathogenesis of Unverricht-Lundborg progressive myoclonus epilepsy (EPM1). *J. Neurobiol.* **56**, 315–327.

Isahara K., Ohsawa Y., Kanamori S., Shibata M., Waguri S., Sato N., Gotow T., Watanabe T., Momoi T., Urase K *et al.* (1999) Regulation of a novel pathway for cell death by lysosomal aspartic and cysteine proteinases. *Neuroscience* **91**, 233–249.

Jeffrey M., Scott J. R., Williams A. and Fraser H. (1992) Ultrastructural features of spongiform encephalopathy transmitted to mice from three species of bovidae. *Acta Neuropathol* **84**, 559–569.

Jellinger K. A. and Stadelmann C. H. (2000) The enigma of cell death in neurodegenerative disorders. *J. Neural Transm. Suppl.* **60**, 21–36.

Kabeya Y., Mizushima N., Ueno T., Yamamoto A., Kirisako T., Noda T., Kominami E., Ohsumi Y. and Yoshimori T. (2000) LC3, a mammalian homologue of yeast Apg8p, is localized in autophagosome membranes after processing. *EMBO J.* **19**, 5720–5728.

Kagedal K., Johansson U. and Ollinger K. (2001) The lysosomal protease cathepsin D mediates apoptosis induced by oxidative stress. *FASEB J.* **15**, 1592–1594.

Kane D. J., Sarafian T. A., Anton R., Hahn H., Butler Gralla E., Selverstone Valentine J., Örd T. and Bredesen D. E. (1993) Bcl-2 inhibition of neuronal death: decreased generation of reactive oxygen species. *Science* **262**, 1274–1277.

Kihara A., Kabeya Y., Ohsumi Y. and Yoshimori T. (2001) Beclin-phosphatidylinositol 3-kinase complex functions at the trans-Golgi network. *EMBO Report* **4**, 330–335.

Klionsky D. J. and Emr S. D. (2000) Autophagy as a regulated pathway of cellular degradation. *Science* **290**, 1717–1721.

Kuan C. Y., Roth K. A., Flavell R. A. and Rakic P. (2000) Mechanisms of programmed cell death in the developing brain. *Trends Neurosci.* **23**, 291–297.

Levi G., Aloisi F., Ciotti M. T. and Gallo V. (1984) Autoradiografic localization and depolarization-induced release of acidic amino-acids in differentiating cerebellar granule cultures. *Brain Res.* **290**, 77–86.

Levy-Strumpf N. and Kimchi A. (1998) Death associated proteins (DAPs): from gene identification to the analysis of their apoptotic and tumor suppressive functions. *Oncogene* **17**, 3331–3340.

Liang X. H. YuJ., Brown K. and Levine B. (2001) Beclin 1 contains a leucine-rich nuclear export signal that is required for its autophagy and tumor suppressor function. *Cancer Res.* **61**, 3443–3449.

Liou W., Geuze H. J., Geelen M. J. and Slot J. W. (1997) The autophagic and endocytic pathways converge at the nascent autophagic vacuoles. *J. Cell Biol.* **136**, 61–70.

Manthrope M., Fagnani R., Skaper S. D. and Varon S. (1986) An automated colorimetric microassay for neuronotrofic factor. *Brain Res.* **390**, 191–198.

Miller T. M., Tansey M. G., Johnson E. M. Jr and Creedon D. J. (1997) Inhibition of phosphatidylinositol 3-kinase activity blocks depolarization-and insulin-like growth factor I-mediated survival of cerebellar granule cells. *J. Biol. Chem.* **272**, 9847–9853.

Munafo D. B. and Colombo M. I. (2001) A novel assay to study autophagy: regulation of autophagosome vacuole size by amino acid deprivation. *J. Cell Sci.* **114**, 3619–3629.

Nakayama M., Ishidoh K., Kayagaki N., Kojima Y., Yamaguchi N., Nakano H., Kominami E., Okumura K. and Yagita H. (2002)

Multiple pathways of TWEAK-induced cell death. *J. Immunol.* **168**, 734–743.

Nardi N., Avidan G., Daily D., Zilkha-Falb R. and Barzilai A. (1997) Biochemical and temporal analysis of events associated with apoptosis induced by lowering the extracellular potassium concentration in mouse cerebellar granule neurons. *J. Neurochem.* **68**, 750–759.

Nitatori T., Sato N., Waguri S., Karasawa Y., Araki H., Shibanai K., Kominami E. and Uchiyama Y. (1995) Delayed neuronal death in the CA1 pyramidal cell layer of the gerbil hippocampus following transient ischemia is apoptosis. *J. Neurosci.* **2**, 1001–1011.

Nixon R. A., Mathews P. M. and Cataldo A. M. (2001) The neuronal endosomal-lysosomal system in Alzheimer's disease. *J. Alzheimers Dis.* **3**, 97–107.

Petiot A., Ogier-Denis E., Blommaart E. F., Meijer A. J. and Codogno P. (2000) Distinct classes of phosphatidylinositol 3′-kinases are involved in signaling pathways that control macroautophagy in HT-29 cells. *J. Biol. Chem.* **275**, 992–998.

Putcha G. V., Harris C. A., Moulder K. L., Easton R. M., Thompson C. B. and Johnson E. M. Jr (2002) Intrinsic and extrinsic pathway signaling during neuronal apoptosis: lessons from the analysis of mutant mice. *J. Cell Biol.* **157**, 441–453.

Saeki K., Yuo A., Okuma E., Yazaki Y., Susin S. A., Kroemer G. and Takaku F. (2000) Bcl-2 down-regulation causes autophagy in a caspase-independent manner in human leukemic HL60 cells. *Cell Death Differ.* **7**, 1263–1269.

Samari H. R. and Seglen P. O. (1998) Inhibition of hepatocytic autophagy by adenosine, aminoimidazole-4-carboxamide riboside, and N6-mercaptopurine riboside. Evidence for involvement of amp-activated protein kinase. *J. Biol. Chem.* **273**, 23 758–23 763.

Schulz J. B., Weller M. and Klockgether T. (1996) Potassium deprivation-induced apoptosis of cerebellar granule neurons. a sequential requirement for new mRNA and protein synthesis, ICE-like protease activity, and reactive oxygen species. *J. Neurosci.* **16**, 4696–4706.

Schwartz L. M., Smith S. W., Jones M. E. and Osborne B. A. (1993) Do all programmed cell deaths occur via apoptosis*? Proc. Natl Acad. Sci. USA* **90**, 80–84.

Schweichel J. U. and Merker H. J. (1973) The morphology of various types of cell death in prenatal tissues. *Teratology* **7**, 253–266.

Seglen P. O. and Gordon P. B. (1982) 3-Methyladenine: specific inhibitor of autophagic/lysosomal protein degradation in isolated rat hepatocytes. *Proc. Natl Acad. Sci. USA* **79**, 1889–1892.

Soto A. M. and Sonnenschein C. (1985) The role of estrogen on the proliferation of human breast tumor cells (MCF-7). *J. Steroid Biochem.* **23**, 87–94.

Stefanis L., Larsen K. E., Rideout H. J., Sulzer D. and Greene L. A. (2001) Expression of A53T mutant but not wild-type alpha-synuclein in PC12 cells induces alterations of the ubiquitin-dependent degradation system, loss of dopamine release, and autophagic cell death. *J. Neurosci.* **21**, 9549–9560.

Stefanis L., Park D. S., Friedman W. J. and Greene L. A. (1999) Caspase-dependent and -independent death of camptothecin-treated embryonic cortical neurons. *J. Neurosci.* **19**, 6235–6247.

Stefanis L., Troy C. M., Qi H. and Greene L. A. (1997) Inhibitors of trypsin-like serine proteases inhibit processing of the caspase Nedd-2 and protect PC12 cells and sympathetic neurons from death evoked by withdrawal of trophic support. *J. Neurochem.* **69**, 1425–1423.

Stoka V. V., Turk B., Schendel S. L., Kim T.-H., Cirman T., Snias S. J., Ellerby L. M., Bredesen D., Freeze H., Abrahamson M. *et al.* (2001) Lysosomal protease pathway to apoptosis: cleavage of bid, not pro-caspase is the most likely route. *J. Biol. Chem.* **276**, 3149–3157.

Stromhaug P. E. and Seglen P. O. (1993) Evidence for acidity of prelysosomal autophagic/endocytic vacuoles (amphisomes). *Biochem. J.* **291**, 115–121.

Subramaniam S., Strelau J. and Unsicker K. (2003) Growth differentiation factor 15 prevents low potassium-induced cell death of cerebellar granule neurons by differential regulation of Akt and ERK pathways. *J. Biol. Chem.* **278**, 8904–8912.

Tanabe H., Eguchi Y., Shimizu S., Martinou J. C. and Tsujimoto Y. (1998) Death-signalling cascade in mouse cerebellar granule neurons. *Eur. J. Neurosci.* **10**, 1043–1411.

Vaillant A. R., Mazzoni I., Tudan C., Boudreau M., Kaplan D. R. and Miller F. D. (1999) Depolarization and neurotrophins converge on the phosphatidylinositol 3-kinase-Akt pathway to synergistically regulate neuronal survival. *J. Cell Biol.* **146**, 955–966.

Villalba M., Bockaert J. and Journot L. (1997) Pituitary adenylate cyclase-activating polypeptide (PACAP-38) protects cerebellar granule neurons from apoptosis by activating the mitogen-activated protein kinase (MAP Kinase) pathway. *J. Neurosci.* **17**, 83–90.

Vitolo O. V., Ciotti M. T., Galli C., Borsello T. and Calissano P. (1998) Adenosine and ADP prevent apoptosis in cultured rat cerebellar granule cells. *Brain Res.* **809**, 297–301.

Volontè C., Ciotti M. T. and Battistini L. (1994) Development of a method for measuring cell number: application to CNS primary neuronal cultures. *Cytometry.* **17**, 274–276.

Watson A., Eilers A., Lallemand D., Kyriakis J., Rubin L. L. and Ham J. (1998) Phosphorylation of c-jun is necessary for apoptosis induced by survival signal withdrawal in cerebellar granule neurons. *J. Neurosci.* **15**, 751–762.

Xue L., Fletcher G. C. and Tolkovsky A. M. (1999) Autophagy is activated by apoptotic signalling in sympathetic neurons: an alternative mechanism of death execution. *Mol Cell Neurosci.* **14**, 180–198.

Yamagishi S., Yamada M., Ishikawa Y., Matsumoto T., Ikeuchi T. and Hatanaka H. (2001) p38 mitogen-activated protein kinase regulates low potassium-induced c-Jun phosphorylation and apoptosis in cultured cerebellar granule neurons. *J. Biol. Chem.* **276**, 5129–5133.

Yasuda Y., Kageyama T., Akamine A., Shibata M., Kominami E., Uchiyama Y. and Yamamoto K. (1999) Characterization of new fluorogenic substrates for the rapid and sensitive assay of cathepsin E and cathepsin D. *J. Biochem.* **125**, 1137–1143.

Zaidi A. U., McDonough J. S., Klocke B. J., Latham C. B., Korsmeyer S. J., Flavell R. A., Schmidt R. E. and Roth K. A. (2001) Chloroquine-induced neuronal cell death is p53 and Bcl-2 family-dependent but caspase-independent. *J. Neuropathol Exp Neurol.* **60**, 937–945.

Zakeri Z., Bursch W., Tenniswood M. and Lockshin R. A. (1995) Programmed, apoptosis, necrosis, or other. *Cell Death Differ.* **2**, 87–96.